

$RE_4B_4O_{11}F_2$ ($RE = \text{Eu, Dy}$):

New Phases Isotypic to the Fluoride Borate $Gd_4B_4O_{11}F_2$

Almut Pitscheider, Michael Enders, and Hubert Huppertz

Institut für Allgemeine, Anorganische und Theoretische Chemie,
Leopold-Franzens-Universität Innsbruck, Innrain 52a, 6020 Innsbruck, Austria

Reprint requests to H. Huppertz. E-mail: Hubert.Huppertz@uibk.ac.at

Z. Naturforsch. **2010**, 65b, 1439 – 1444; received September 17, 2010

The rare-earth fluoride borates $RE_4B_4O_{11}F_2$ ($RE = \text{Eu, Dy}$) were synthesized in a Walker-type multianvil apparatus from the corresponding rare-earth oxides and fluorides, and boron oxide. $Eu_4B_4O_{11}F_2$ was obtained under high-pressure/high-temperature conditions of 5 GPa and 900 °C, and $Dy_4B_4O_{11}F_2$ at 8 GPa and 1000 °C. The single-crystal structure determinations revealed that both compounds are isotypic to $Gd_4B_4O_{11}F_2$, crystallizing in the space group $C2/c$ ($Z = 4$) with the parameters $a = 1368.2(3)$, $b = 465.4(1)$, $c = 1376.6(3)$ pm, $\beta = 91.2(1)^\circ$, $V = 0.8765(3)$ nm³, $R_1 = 0.0232$, and $wR_2 = 0.0539$ (all data) for $Eu_4B_4O_{11}F_2$ and $a = 1349.5(3)$, $b = 460.9(1)$, $c = 1362.5(3)$ pm, $\beta = 91.3(1)^\circ$, $V = 0.8472(3)$ nm³, $R_1 = 0.0353$, and $wR_2 = 0.0729$ (all data) for $Dy_4B_4O_{11}F_2$. These phases are entirely different from the recently discovered lanthanum fluoride borate $La_4B_4O_{11}F_2$, which exhibits the same constitution in another structure type with space group $P2_1/c$.

Key words: Rare Earth, Fluoride, Borate, High Pressure, Crystal Structure

Introduction

Considering the extensive research on oxoborates under high-pressure/high-temperature conditions in our group in the last decade, it was tempting to extend our investigations into fluoride borates. These compounds, especially “fluoroborate” glasses, have been the subject of much recent work, but crystalline fluorido and fluoride borates have not been that well studied, except for natural minerals with more than two cations. The difference between fluorido borates (old designation: fluoroborates) and fluoride borates lies in the coordination sphere of boron. While borates, that contain only isolated fluorine anions, are generally termed “fluoride borates”, “fluorido borates” contain fluorine atoms covalently bound to the boron atoms. Due to the structural similarities of fluoride borates to oxoborates, it is more than likely that numerous new compounds and crystal structures with interesting physical properties can be obtained in the field of fluoride borates under pressure. A summary of the achievements reached so far can be found in [1].

For the composition $RE_4B_4O_{11}F_2$, two different structure types were obtained by high-pressure/high-temperature synthesis up to now. The recently presented compound $La_4B_4O_{11}F_2$ [2] crystallizes in the space group $P2_1/c$ with the lattice parameters

$a = 778.1(2)$, $b = 3573.3(7)$, $c = 765.7(2)$ pm, and $\beta = 113.92(3)^\circ$ ($Z = 8$). The crystal structure consists of BO_3 groups (\triangle), which are either isolated (\triangle), connected *via* common corners ($\triangle\triangle$), or connected *via* a BO_4 tetrahedron, forming a fundamental building block (FBB) $2\triangle\triangle\triangle$: $\triangle\triangle\triangle$.

The fluoride borate $Gd_4B_4O_{11}F_2$ discovered earlier shows the same atomic composition, except for a completely different crystal structure in the space group $C2/c$ [3]. In the crystal structure of $Gd_4B_4O_{11}F_2$, there are BO_3 groups and BO_4 tetrahedra, connected *via* common corners. The structural motif consists of two BO_3 groups (\triangle) and two BO_4 tetrahedra (\square), and can be described with the fundamental building block $2\triangle\triangle\square$: $\triangle\square\square\triangle$ (after Burns *et al.* [4]), which represents a novelty in borate chemistry.

Here we report about two new compounds $RE_4B_4O_{11}F_2$ ($RE = \text{Eu, Dy}$), which are isotypic to $Gd_4B_4O_{11}F_2$. The syntheses and crystal structures of $RE_4B_4O_{11}F_2$ ($RE = \text{Eu, Dy}$) are presented in comparison to $Gd_4B_4O_{11}F_2$.

Experimental Section

Syntheses

For the syntheses of $RE_4B_4O_{11}F_2$ ($RE = \text{Eu, Dy}$), the reactions of the oxides RE_2O_3 ($RE = \text{Eu, Dy}$) and

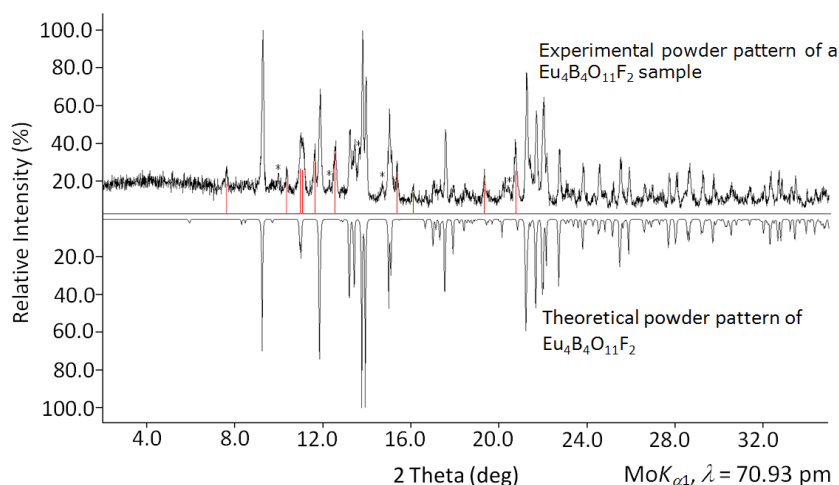


Fig. 1 (color online). Top: experimental powder pattern of $Eu_4B_4O_{11}F_2$; the reflections of EuF_3 and an unknown phase are indicated with lines and asterisks, respectively. Bottom: theoretical powder pattern of $Eu_4B_4O_{11}F_2$, based on single-crystal diffraction data.

B_2O_3 with the corresponding rare-earth fluoride REF_3 were performed under high-pressure/high-temperature conditions. For $Eu_4B_4O_{11}F_2$, the synthesis was carried out at 5 GPa and 900 °C, while $Dy_4B_4O_{11}F_2$ was obtained at 8 GPa and 1000 °C. Mixtures of Eu_2O_3 (Smart Elements, 99.99 %) or Dy_2O_3 (Strem Chemicals, 99.9 %), B_2O_3 (Strem Chemicals, 99.9+ %), and EuF_3 (Strem Chemicals, 99.9 %) or DyF_3 (Strem Chemicals, 99.9 %) with a molar ratio of 1:1:3 were ground inside of a glove box and filled into boron nitride crucibles (Henze BNP GmbH, HeBoSint® S100, Kempen, Germany). These crucibles were placed into the center of 18/11-assemblies, which were compressed by eight tungsten carbide cubes (TSM-10 Ceratizit, Reutte, Austria). The details of preparing the assemblies can be found in refs. [5–9]. Pressure was applied by a multianvil device, based on a Walker-type module and a 1000 ton press (both devices from the company Voggenreiter, Mainleus, Germany). For the syntheses of $Eu_4B_4O_{11}F_2$ / $Dy_4B_4O_{11}F_2$ the educts were compressed up to 5 / 8 GPa in 130 / 220 min, then heated to 900 / 1000 °C in 15 min, and kept there for 20 min. Afterwards, the temperature was lowered to 700 / 750 °C in 20 min, and finally to r.t. by switching off the heating. The decompression of the assemblies required 390 / 660 min. The recovered MgO octahedra (pressure-transmitting medium, Ceramic Substrates & Components Ltd., Newport, Isle of Wight, UK) were broken apart and the samples carefully separated from the surrounding boron nitride crucibles. Colorless, air- and water-resistant crystals of $Eu_4B_4O_{11}F_2$ and $Dy_4B_4O_{11}F_2$ were the products of the respective syntheses.

Since the syntheses were initially planned to give fluorine-rich borates an excess of rare-earth fluoride was always applied ($RE_2O_3 : B_2O_3 : REF_3 = 1 : 1 : 3$; the ideal ratio for the syntheses of the composition $RE_4B_4O_{11}F_2$ is 5:6:2). Notwithstanding, the products contained mainly the compounds $RE_4B_4O_{11}F_2$ ($RE = Eu, Dy$) besides remaining REF_3

and yet unidentified phases. Obviously, this composition and the associated $Gd_4B_4O_{11}F_2$ structure type seem to have a remarkable tendency towards formation under these extreme conditions.

Crystal structure analyses

$Eu_4B_4O_{11}F_2$ was identified by X-ray powder diffraction on a flat sample of the reaction product, using a Stoe Stadi P powder diffractometer with $MoK_{\alpha 1}$ radiation (transmission geometry, Ge monochromator, $\lambda = 70.93$ pm). Fig. 1 shows the powder pattern, displaying $Eu_4B_4O_{11}F_2$ as well as reflections of the excess educt EuF_3 (marked with lines in Fig. 1). Additional reflections, which could not be assigned to a known phase, are marked with asterisks. The experimental powder pattern (top) is in good agreement with the theoretical pattern (bottom), simulated from the single-crystal data. By indexing the reflections of the europium fluoride borate, the parameters $a = 1368.2(3)$, $b = 465.3(2)$, $c = 1376.8(3)$ pm, $\beta = 91.2(2)^\circ$ with a volume of $0.8762(3)$ nm³ were obtained. This validated the lattice parameters received from the single-crystal X-ray diffraction data (Table 1). The intensity data of single crystals of both $Eu_4B_4O_{11}F_2$ and $Dy_4B_4O_{11}F_2$ were collected at r.t. by use of a Kappa CCD diffractometer (Bruker AXS / Nonius, Karlsruhe), equipped with a Miracol fiber optics collimator and a Nonius FR590 generator (graphite-monochromatized MoK_{α} radiation, $\lambda = 71.073$ pm). Absorption corrections, based on multi-scans, were performed with SCALEPACK [10]. All significant details of the data collections and analyses are listed in Table 1. For the structural refinement, the positional parameters of the isotopic compound $Gd_4B_4O_{11}F_2$ were used as starting values [3]. The parameter refinements (full-matrix least-squares against F^2) were achieved by using the SHELX-97 software suite [11, 12]. All atoms were refined with anisotropic atomic displace-

Table 1. Crystal data and structure refinement of $RE_4B_4O_{11}F_2$ ($RE = \text{Eu, Dy}$) (standard deviations in parentheses).

Empirical formula	$\text{Eu}_4\text{B}_4\text{O}_{11}\text{F}_2$	$\text{Dy}_4\text{B}_4\text{O}_{11}\text{F}_2$
Molar mass, g mol^{-1}	865.08	907.24
Crystal system	monoclinic	
Space group	$C2/c$	
Powder diffractometer	Stoe Stadi P	
Radiation; λ , pm	$\text{MoK}\alpha_1$; 70.93	
	(Ge(111) monochromator)	
Powder data		
a , pm	1368.2(3)	
b , pm	465.3(2)	
c , pm	1376.8(3)	
β , deg	91.2(2)	
V , nm^3	0.8762(3)	
Single-crystal diffractometer	Nonius Kappa CCD	
Radiation; λ , pm	$\text{MoK}\alpha$; 71.073	
	(graphite monochromator)	
Single-crystal data		
a , pm	1368.2(3)	1349.5(3)
b , pm	465.4(1)	460.9(1)
c , pm	1376.6(3)	1362.5(3)
β , deg	91.2(1)	91.3(1)
V , nm^3	0.8765(3)	0.8472(3)
Formula units per cell	$Z = 4$	$Z = 4$
Calcd density, g cm^{-3}	6.56	7.11
$F(000)$, e	1512	1560
Temperature, K	293(2)	293(2)
Crystal size, mm^3	$0.04 \times 0.04 \times 0.07$	$0.03 \times 0.04 \times 0.05$
Absorption coeff, mm^{-1}	28.3	35.0
Absorption correction	multi-scan	multi-scan
θ range, deg	3.0–32.5	3.0–32.5
Range in hkl	$-18/+20, \pm 7, \pm 20$	$-20/+18, \pm 6, \pm 20$
Total no. of reflections	5011	5261
Independent refls / R_{int}	1576 / 0.0494	1533 / 0.0544
Refls with $I \geq 2\sigma(I) / R_\sigma$	1454 / 0.0374	1331 / 0.0394
Data / ref. parameters	1576 / 97	1533 / 97
Goodness-of-fit on F^2	1.156	1.098
Final indices R_1/wR_2	0.0210 / 0.0529	0.0288 / 0.0702
$[I \geq 2\sigma(I)]$		
Indices R_1/wR_2 (all data)	0.0232 / 0.0539	0.0353 / 0.0729
Largest diff. peak / hole, $\times 10^{-6} \text{ e pm}^{-3}$	3.2 / -2.0	3.8 / -2.3

ment parameters. The final difference Fourier syntheses did not reveal any significant residual peaks in all refinements. The positional parameters of the atom refinements, interatomic distances, and interatomic angles are listed in the Tables 2–4.

Further details of the crystal structure investigation may be obtained from Fachinformationszentrum Karlsruhe, 76344 Eggenstein-Leopoldshafen, Germany (fax: +49-7247-808-666; e-mail: crysdata@fiz-karlsruhe.de, http://www.fiz-informationsdienste.de/en/DB/icsd/depot_anforderung.html) on quoting the deposition number CSD-422159 ($\text{Eu}_4\text{B}_4\text{O}_{11}\text{F}_2$) and CSD-422160 ($\text{Dy}_4\text{B}_4\text{O}_{11}\text{F}_2$).

Table 2. Atomic coordinates and isotropic equivalent displacement parameters U_{eq} for $RE_4B_4O_{11}F_2$ ($RE = \text{Eu, Dy}$) (space group: $C2/c$) (standard deviations in parentheses). U_{eq} is defined as one third of the trace of the orthogonalized U_{ij} tensor.

Atom	W. position	x	y	z	U_{eq} (\AA^2)
Eu1	8f	0.05887(2)	0.52031(4)	0.37058(2)	0.00489(8)
Eu2	8f	0.27958(2)	0.01747(4)	0.37066(2)	0.00456(8)
B1	8f	0.9070(3)	0.9774(8)	0.2857(3)	0.0052(7)
B2	8f	0.0953(3)	0.9557(8)	0.5251(3)	0.0052(6)
O1	8f	0.9122(2)	0.8673(5)	0.3937(2)	0.0053(4)
O2	8f	0.1736(2)	0.8139(5)	0.2577(2)	0.0061(4)
O3	8f	0.0790(2)	0.6653(5)	0.5351(2)	0.0063(4)
O4	4e	0	0.8476(7)	1/4	0.0046(6)
O5	8f	0.1146(2)	0.0609(6)	0.4348(2)	0.0078(5)
O6	8f	0.9012(2)	0.2796(5)	0.2751(2)	0.0064(4)
F1	8f	0.2308(2)	0.5244(5)	0.4248(2)	0.0114(5)
Dy1	8f	0.05887(2)	0.51733(5)	0.37032(2)	0.0063(2)
Dy2	8f	0.28029(2)	0.01473(5)	0.37012(2)	0.0058(2)
B1	8f	0.9065(5)	0.974(2)	0.2867(5)	0.006(2)
B2	8f	0.0963(5)	0.958(2)	0.5226(5)	0.009(2)
O1	8f	0.9122(2)	0.8625(8)	0.3952(3)	0.0055(6)
O2	8f	0.1761(2)	0.8147(8)	0.2576(3)	0.0066(7)
O3	8f	0.0786(3)	0.6664(8)	0.5335(3)	0.0069(7)
O4	4e	0	0.841(2)	1/4	0.0059(9)
O5	8f	0.1156(3)	0.634(8)	0.4322(3)	0.0078(7)
O6	8f	0.9015(3)	0.2795(8)	0.2763(3)	0.0074(7)
F1	8f	0.2312(3)	0.5272(7)	0.4244(3)	0.0127(7)

Results and Discussion

The structures of $RE_4B_4O_{11}F_2$ ($RE = \text{Eu, Dy}$) contain BO_3 groups and BO_4 tetrahedra, connected via common corners (Fig. 2). The main structural motif

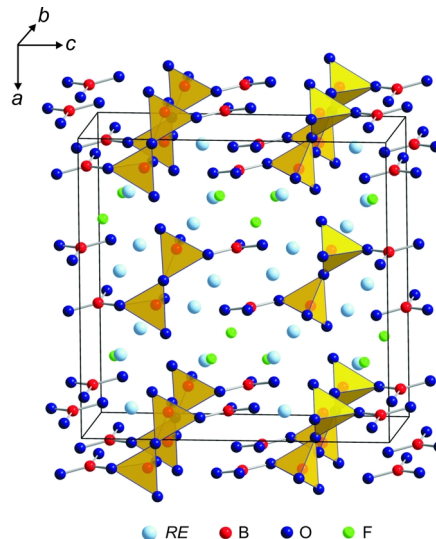


Fig. 2 (color online). Crystal structure of $RE_4B_4O_{11}F_2$ ($RE = \text{Eu, Gd, Dy}$), showing the fundamental building block $2\Delta 2\Box$: $\Delta\Box\Box\Delta$.

Eu1–O6a	237.1(2)	Eu2–O2a	230.7(2)	B1–O6	141.6(4)
Eu1–O3a	237.4(2)	Eu2–O2b	234.2(2)	B1–O2	145.8(5)
Eu1–O4	238.1(2)	Eu2–O6	241.1(2)	B1–O4	150.1(4)
Eu1–O5a	243.0(3)	Eu2–O5	244.9(3)	B1–O1	157.3(5)
Eu1–F1	245.3(3)	Eu2–O1	245.4(2)		av. = 148.7
Eu1–O3b	246.8(2)	Eu2–O3	246.0(2)		
Eu1–O1	260.1(2)	Eu2–F1a	250.8(2)	B2–O5	136.7(5)
Eu1–O2	261.6(3)	Eu2–F1b	256.7(2)	B2–O3	137.7(4)
Eu1–O6b	274.2(2)	Eu2–F1c	282.9(3)	B2–O1	139.4(5)
Eu1–O5b	276.9(3)		av. = 248.1		av. = 137.9
	av. = 252.1				
F1–Eu1	245.3(3)				
F1–Eu2a	250.8(2)				
F1–Eu2b	256.7(2)				
F1–Eu2c	282.9(3)				
	av. = 258.9				
Dy1–O3a	233.6(4)	Dy2–O2a	225.3(4)	B1–O6	141.5(7)
Dy1–O4	234.2(4)	Dy2–O2b	230.9(4)	B1–O2	145.6(8)
Dy1–O6a	235.1(4)	Dy2–O6	236.3(4)	B1–O4	149.9(7)
Dy1–O5a	237.5(4)	Dy2–O5	240.6(4)	B1–O1	156.6(8)
Dy1–F1	242.3(4)	Dy2–O1	241.3(4)		av. = 148.4
Dy1–O3b	244.7(4)	Dy2–O3	243.5(4)		
Dy1–O1	256.8(4)	Dy2–F1a	246.1(3)	B2–O5	135.7(8)
Dy1–O2	261.8(4)	Dy2–F1b	256.7(3)	B2–O3	137.1(7)
Dy1–O6b	268.8(4)	Dy2–F1c	281.4(5)	B2–O1	140.0(8)
Dy1–O5b	275.7(4)		av. = 244.7		av. = 137.6
	av. = 249.1				
F1–Dy1	242.3(4)				
F1–Dy2a	246.1(3)				
F1–Dy2b	256.7(3)				
F1–Dy2c	281.4(5)				
	av. = 256.6				

Table 3. Interatomic distances (pm) in $RE_4B_4O_{11}F_2$ ($RE = Eu, Dy$) (space group: $C2/c$), calculated with the single-crystal lattice parameters (standard deviations in parentheses).

O6–B1–O2	115.9(3)	O5–B2–O3	118.5(3)	Eu1–F1–Eu2a	100.2(1)
O6–B1–O4	114.3(3)	O5–B2–O1	122.4(3)	Eu1–F1–Eu2b	99.1(1)
O2–B1–O4	107.2(3)	O3–B2–O1	119.0(3)	Eu1–F1–Eu2c	103.6(1)
O6–B1–O1	115.0(3)		av. = 120.0	Eu2a–F1–Eu2b	133.0(2)
O2–B1–O1	103.7(3)			Eu2a–F1–Eu2c	112.2(1)
O4–B1–O1	99.0(3)			Eu2b–F1–Eu2c	104.1(1)
	av. = 109.2				av. = 108.7
O6–B1–O2	115.3(5)	O5–B2–O3	119.2(6)	Dy1–F1–Dy2a	100.9(2)
O6–B1–O4	114.4(5)	O5–B2–O1	122.3(5)	Dy1–F1–Dy2b	98.4(2)
O2–B1–O4	107.3(4)	O3–B2–O1	118.4(6)	Dy1–F1–Dy2c	103.1(2)
O6–B1–O1	115.0(5)		av. = 120.0	Dy2a–F1–Dy2b	132.8(3)
O2–B1–O1	104.1(4)			Dy2a–F1–Dy2c	112.5(2)
O4–B1–O1	99.0(4)			Dy2b–F1–Dy2c	104.1(2)
	av. = 109.2				av. = 108.6

Table 4. Interatomic angles (deg) in $RE_4B_4O_{11}F_2$ ($RE = Eu, Dy$) (space group: $C2/c$), calculated with the single-crystal lattice parameters (standard deviations in parentheses).

consists of two BO_3 groups (\triangle) and two BO_4 tetrahedra (\square), which can be described with the fundamental building block $2\triangle 2\square$: $\triangle\square\square\triangle$ (after Burns *et al.* [4]), a novelty in borate chemistry. For a detailed depiction of the structure, the reader is referred to the description of the isotypic compound $Gd_4B_4O_{11}F_2$ [3]. In this paper, a comparison of the three isotypic compounds $RE_4B_4O_{11}F_2$ ($RE = Eu, Gd, Dy$) is given.

Fig. 3 shows a comparison of the values of the lattice parameters of $Eu_4B_4O_{11}F_2$, $Gd_4B_4O_{11}F_2$ [3], and $Dy_4B_4O_{11}F_2$. The exact values are given in Table 5. The difference of the lattice parameters corresponds to the decreasing ionic radii (lanthanoid contraction) of the rare-earth cations. The values for the ionic radius of ninefold coordinated cations are taken from reference [13]: Eu^{3+} (126.0 pm), Gd^{3+} (124.7 pm), and Dy^{3+} (122.3 pm). Because the size differences

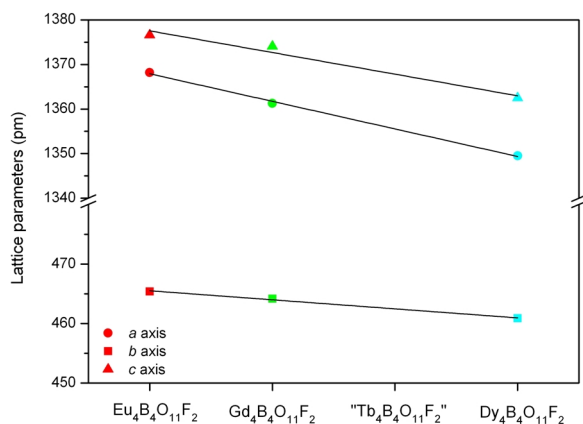


Fig. 3 (color online). Visualization of the progression of the lattice parameters (pm) of $RE_4B_4O_{11}F_2$ ($RE = \text{Eu, Gd, Dy}$) with the decrease due to the lanthanoid contraction.

are not too large, the bond lengths and angles of $RE_4B_4O_{11}F_2$ ($RE = \text{Eu, Dy}$) are comparable to the values found in $Gd_4B_4O_{11}F_2$ [3]. The Eu–O/F distances are in the range 230.7(2)–282.9(3) pm and the Dy–O/F distances within 225.3(4)–281.4(5) pm. This fits well to the values of 230.0(3)–283.7(3) pm for Gd–O/F in $Gd_4B_4O_{11}F_2$. The mean Gd–F distance is 258.4 pm, which lies between the mean RE –F bond lengths of 258.9 and 256.6 pm in $Eu_4B_4O_{11}F_2$ and $Dy_4B_4O_{11}F_2$, respectively. In the crystal structure of $Gd_4B_4O_{11}F_2$, a distorted tetrahedron was found and interpreted as a BO_3 group, in which the boron atom is drawn towards a fourth oxygen atom, resulting in a long B–O bond [3]. For $Gd_4B_4O_{11}F_2$, this long B1–O1 bond measures 159.0(6) pm. The corresponding B–O distances in $Eu_4B_4O_{11}F_2$ and $Dy_4B_4O_{11}F_2$ are slightly shorter with values of 157.3(5) and 156.6(8) pm, respectively. Inside the BO_3 groups of these structures, average B–O distances of 137.9 and 137.6 pm are found for $RE_4B_4O_{11}F_2$ ($RE = \text{Eu, Dy}$) – in perfect agreement with the literature.

We also calculated the charge distribution of the atoms in $RE_4B_4O_{11}F_2$ ($RE = \text{Eu, Dy}$) *via* bond valence sums (ΣV), using VALIST (Bond Valence Calculation and Listing) [14] and the CHARDI (*charge distribution in solids*) concept (ΣQ) [15–17], verifying the formal valence states in the fluoride borates. Table 6 shows the formal ionic charges, received from the calculations, which correspond to the expected values.

Additionally, we calculated the MAPLE values (*Madelung Part of Lattice Energy* according to Hoppe [18–20]) of $RE_4B_4O_{11}F_2$ ($RE =$

Table 5. Comparison of the single-crystal lattice parameters and volumes of $RE_4B_4O_{11}F_2$ ($RE = \text{Eu, Gd, Dy}$) (standard deviations in parentheses).

Compound	<i>a</i> (pm)	<i>b</i> (pm)	<i>c</i> (pm)	β (deg)	<i>V</i> (nm ³)
$Eu_4B_4O_{11}F_2$	1368.2(3)	465.4(1)	1376.6(3)	91.2(1)	0.8765(3)
$Gd_4B_4O_{11}F_2$	1361.3(3)	464.2(2)	1374.1(3)	91.3(1)	0.8681(3)
$Dy_4B_4O_{11}F_2$	1349.5(3)	460.9(1)	1362.5(3)	91.3(1)	0.8472(3)

Table 6. Charge distribution in $RE_4B_4O_{11}F_2$ ($RE = \text{Eu, Dy}$), calculated with VALIST (ΣV) [17] and the CHARDI concept (ΣQ) [18–20].

	Dy1	Dy2	B1	B2	Eu1	Eu2	B1	B2
ΣV	2.80	2.79	2.98	2.96	3.11	3.01	2.96	2.94
ΣQ	2.98	3.06	2.96	3.00	2.98	3.04	2.97	3.01
	O1	O2	O3	O4	O1	O2	O3	O4
ΣV	–2.06	–1.93	–2.01	–2.21	–2.12	–2.04	–2.13	–1.84
ΣQ	–2.00	–1.98	–2.12	–2.25	–2.00	–2.00	–2.10	–2.22
	O5	O6	F1		O5	O6	F1	
ΣV	–1.87	–1.81	–0.76		–1.91	–1.90	–0.97	
ΣQ	–1.90	–1.94	–0.94		–1.90	–1.92	–0.98	

Eu, Dy), which were checked against the data of the binary compounds. We obtained a value of 72337 kJ mol^{–1} for $Eu_4B_4O_{11}F_2$, to be compared with 72620 kJ mol^{–1} (deviation: 0.4 %), based on the binary components [$5/3 \times Eu_2O_3$ (14991 kJ mol^{–1} [21]) + $2 \times B_2O_3$ –I (21938 kJ mol^{–1} [22]) + $2/3 \times EuF_3$ (5797 kJ mol^{–1} [23])]. For $Dy_4B_4O_{11}F_2$, the resulting value is 72799 kJ mol^{–1}, compared to 73179 kJ mol^{–1} (deviation: 0.5 %) based on the binary components [$5/3 \times Dy_2O_3$ (14991 kJ mol^{–1} [24]) + $2 \times B_2O_3$ –I (21938 kJ mol^{–1} [22]) + $2/3 \times DyF_3$ (5797 kJ mol^{–1} [23])].

Conclusion

With the synthesis of $RE_4B_4O_{11}F_2$ ($RE = \text{Eu, Dy}$), the range of compounds with the composition $RE_4B_4O_{11}F_2$ has been extended and explored in more detail. The existence of the isotypic compound “ $Tb_4B_4O_{11}F_2$ ” still missing in the series is very likely; further studies on this phase and the possible formation of $RE_4B_4O_{11}F_2$ with $RE = \text{Ho–Lu}$ are planned. Additional experiments with the larger rare-earth cations $RE = \text{Ce–Nd}$ and Sm will be performed to investigate the transformation into the structure type of $La_4B_4O_{11}F_2$ and any polymorphs.

Acknowledgement

We would like to thank Dr. G. Heymann for collecting the single-crystal data.

- [1] H. Huppertz, *Chem. Commun.* **2011**, DOI:10.1039/C0CC02715D.
- [2] A. Haberer, R. Kaindl, O. Oeckler, H. Huppertz, *J. Solid State Chem.* **2010**, *183*, 1970.
- [3] A. Haberer, R. Kaindl, H. Huppertz, *J. Solid State Chem.* **2010**, *183*, 471.
- [4] P.C. Burns, J.D. Grice, F.C. Hawthorne, *Can. Mineral.* **1995**, *33*, 1131.
- [5] D. Walker, M. A. Carpenter, C. M. Hitch, *Am. Mineral.* **1990**, *75*, 1020.
- [6] D. Walker, *Am. Mineral.* **1991**, *76*, 1092.
- [7] H. Huppertz, *Z. Kristallogr.* **2004**, *219*, 330.
- [8] D. C. Rubie, *Phase Transitions* **1999**, *68*, 431.
- [9] N. Kawai, S. Endo, *Rev. Sci. Instrum.* **1970**, *8*, 1178.
- [10] SCALEPACK. Z. Otwinowski, W. Minor in *Methods in Enzymology*, Vol. 276, *Macromolecular Crystallography*, Part A (Eds.: C. W. Carter Jr., R. M. Sweet), Academic Press, New York, **1997**, pp. 307.
- [11] G.M. Sheldrick, SHELXS/L-97, Programs for Crystal Structure Determination, University of Göttingen, Göttingen (Germany) **1997**.
- [12] G.M. Sheldrick, *Acta Crystallogr.* **2008**, *A64*, 112.
- [13] R.D. Shannon, *Acta Crystallogr.* **1976**, *A32*, 751.
- [14] A. S. Wills, VALIST (version 4.0.0), University College London, London (U. K.) **1998–2008**; program available from www.ccp14.ac.uk.
- [15] I. D. Brown, D. Altermatt, *Acta Crystallogr.* **1985**, *B41*, 244.
- [16] N. E. Brese, M. O’Keeffe, *Acta Crystallogr.* **1991**, *B47*, 192.
- [17] R. Hoppe, S. Voigt, H. Glaum, J. Kissel, H. P. Müller, K. J. Bernet, *J. Less-Common Met.* **1989**, *156*, 105.
- [18] R. Hoppe, *Angew. Chem.* **1966**, *78*, 52; *Angew. Chem., Int. Ed. Engl.* **1966**, *5*, 96.
- [19] R. Hoppe, *Angew. Chem.* **1970**, *82*, 7; *Angew. Chem., Int. Ed. Engl.* **1970**, *9*, 25.
- [20] R. Hübenthal, M. Serafin, R. Hoppe, MAPLE (version 4.0), Program for the Calculation of Distances, Angles, Effective Coordination Numbers, Coordination Spheres, and Lattice Energies, University of Gießen, Gießen (Germany) **1993**.
- [21] D. H. Templeton, C. H. Dauben, *J. Am. Chem. Soc.* **1954**, *76*, 5237.
- [22] C. T. Prewitt, R. D. Shannon, *Acta Crystallogr.* **1968**, *B24*, 869.
- [23] A. Zalkin, D. H. Templeton, *J. Am. Chem. Soc.* **1953**, *75*, 2453.
- [24] P. Karen, *J. Solid State Chem.* **2004**, *177*, 281.